

Bi-level Optimal Planning of Voltage Regulator in Distribution Systems Considering Maximization of Incentive-based Photovoltaic Energy Integration

Xu Xu, *Member, IEEE*, Youwei Jia[✉], *Member, IEEE*, Chun Sing Lai, *Member, IEEE*, Minghao Wang, *Member, IEEE*, and Zhao Xu, *Senior Member, IEEE*

Abstract—This paper focuses on optimal voltage regulator (VR) planning to maximize the photovoltaic (PV) energy integration in distribution grids. To describe the amount of dynamic PV energy that can be integrated into the power system, the concept of PV accommodation capability (PVAC) is introduced and modeled with optimization. Our proposed planning model is formulated as a Benders decomposition based bi-level stochastic optimization problem. In the upper-level problem, VR planning decisions and PVAC are determined via mixed integer linear programming (MILP) before considering uncertainty. Then in the lower-level problem, the feasibility of first-level results is checked by critical network constraints (e.g. voltage magnitude constraints and line capacity constraints) under uncertainties considered by time-varying loads and PV generations. In this paper, these uncertainties are represented in the form of operational scenarios, which are generated by the Gaussian copula theory and reduced by a well-studied backward-reduction algorithm. The modified IEEE 33-node distribution grid is utilized to verify the effectiveness of the proposed model. The results demonstrate that a PV energy integration can be significantly enhanced after optimal voltage regulator planning.

Index Terms—Bi-level stochastic optimization problem, critical network constraints, photovoltaic energy integration, uncertainties, voltage regulator planning.

Manuscript received April 11, 2020; revised June 29, 2020; accepted July 23, 2020. Date of online publication August 19, 2020; date of current version June 15, 2022. This work is partially supported by Natural Science Foundation of Guangdong (2019A1515111173), Young Talent Program (Dept of Education of Guangdong) (2018KQNCX223), High-level University Fund, G02236002, National Natural Science Foundation of China (71971183) and Hong Kong UGC PolyU Grant under Project P0038972.

X. Xu is with Department of Electrical and Electronic Engineering, Southern University of Science and Technology, Shenzhen, China; and also with Department of Electrical Engineering, The Hong Kong Polytechnic University, Hung Hom, Hong Kong SAR, China.

Y. W. Jia (corresponding author, email: jiayw@sustech.edu.cn, ORCID: <https://orcid.org/0000-0003-3071-5552>) is with Department of Electrical and Electronic Engineering, and University Key Laboratory of Advanced Wireless Communications of Guangdong Province, Southern University of Science and Technology, Shenzhen 515100, China.

C. S. Lai is with Brunel Institute of Power Systems, Department of Electronic and Computer Engineering, Brunel University London, London, UB8 3PH, United Kingdom.

M. H. Wang is with the Department of Electrical Engineering, The Hong Kong Polytechnic University, Hung Hom, Hong Kong SAR, China.

Z. Xu is with both Shenzhen Research Institute and Department of Electrical Engineering, The Hong Kong Polytechnic University, Hung Hom, Hong Kong SAR, China.

DOI: 10.17775/CSEEJPES.2020.01230

NOMENCLATURE

| | |
|---|---|
| t/T | Index/set of times. |
| w/W | Index/set of uncertainty scenarios. |
| j/J | Index/set of nodes. |
| $i/\phi(j)$ | Index/set of child nodes. |
| α | Index of piecewise linearization approximation method. |
| $\Omega^{\text{AP}}/\Omega^{\text{RP}}$ | Sets for the quadratic term representing active/reactive power. |
| Q_{jtw}^{PV} | Reactive PV output. |
| V_{jtw} | Node voltage magnitude. |
| \bar{V}_{jtw} | Voltage magnitude at the point of VR installation. |
| P_{jtw}/Q_{jtw} | Active/Reactive power flow. |
| $P_{jtw}^{\text{QT}}/Q_{jtw}^{\text{QT}}$ | Quadratic terms of active/reactive power flow. |
| u_j^{VR} | Binary decision variable for VR installation status. |
| u_j^{PV} | Binary decision variable for PV energy connection. |
| E_j^{PV} | Size of PV energy integration. |
| Z_j^{PV} | Auxiliary variable representing the bilinear term. |
| $s_{jtw}^{\text{V, LB}}/s_{jtw}^{\text{V, UB}}$ | Slack variables for voltage constraints. |
| s_{jtw}^{PQ} | Slack variable for line capacity constraints. |
| c_{inv}^{VR} | VR investment cost (\$). |
| $c_{o\&m}^{\text{VR}}$ | VR operating and maintenance cost (\$/day). |
| c^{PV} | Subsidy for PV generation integration. |
| c^{Penalty} | Penalty coefficient for voltage deviation and overload (\$/p.u.). |
| p_w | Probability of scenario. |
| C^{VR} | VR planning budget. |
| μ_{tw}^{PV} | PV generation factor (ratio of the PV accommodation capability). |
| κ | Daily capital recovery factor for VR. |
| r_{ij}/x_{ij} | Resistance/Reactance of the distribution line. |
| θ^{PV} | Power factor angle for PV power systems. |
| p_{jtw}/q_{jtw} | Active/Reactive load. |
| V/\bar{V} | Minimum/Maximum voltage magnitude. |
| \bar{P}/\bar{Q} | Maximum active/reactive power flow. |
| LC_{ij}/SC | Distribution line/Substation capacity. |
| \bar{Q}^{PV} | Upper bound of reactive PV output. |

I. INTRODUCTION

AS an emerging solution to solve the energy crisis and reduce greenhouse gas emission, a distributed photovoltaic (PV) generation system has become very popular in recent years [1]–[5]. In this paper, we investigate the financial incentives (or monetary benefit) for PV energy integration. The concept of “incentive-based PV energy integration” can be construed as subsidy-based PV energy integration. Under this mechanism, the owner of PV generators, i.e., the distribution system operators, receive a certain amount of financial reward for providing PV energy to the power grid. The distribution system operator is motivated to accept an incentive program in which they see additional revenue sources [6], [7]. However, the uncertain PV output presents significant uncertainties to the power grids. In addition, the over-proliferation of PV generators brings about various negative effects on normal operating conditions for grids [8], which directly affects the capability of hosting PV integration. In this regard, the grid planners need a reasonable and effective method to improve the PV energy integration to ensure no violations of normal distribution grid operation constraints [9], especially voltage magnitude violations and line capacity violations.

In this paper, PV accommodation capability (PVAC) is introduced to describe how much PV generations can be accommodated by a grid within a certain time slot. Several methods have been proposed to improve PV energy penetration in the distribution grids. One of the popular methods is based on Monte Carlo simulation [10], where stochastic analysis is presented to evaluate the PVAC. Other methods are based on optimization techniques, which have many real-life applications in different fields, such as [11]–[16]. In addition, an optimization-based method is proposed in [17] to consider both technical and economic aspects of renewable hosting capacity enhancement. There are many real-life applications of optimization techniques in different fields. For example, the study in [18] presents a method to increase the PV hosting capacity of the low-voltage network. The method consists of voltage droop control to efficiently control the active medium-voltage to low-voltage transformers in the condition of high PV energy integration. To facilitate the integration of solar PV in small-scale systems, optimal scheduling regimes (e.g. [19]) and specific energy management methods (e.g. [20], [21]) can be employed to settle the induced uncertainties. From a demand response perspective, reference [22] provides a multi-objective and multi-period nonlinear programming optimization model, where the demand response is utilized to enhance the system’s ability to hold PV generations and decrease the active power losses at the sametime. In [23], in terms of voltage sensitivity analysis results, a novel voltage control method is developed to improve the accommodation capability of PV energy via energy storage system management. Reference [24] aims to improve the renewable hosting capacity by optimal coordinated operation of the on-load tap changer and static var compensators in the distribution system. Nevertheless, to improve renewable accommodation capability, most of the existing works only study short-term operational strategies rather than considering long-term planning of advanced devices, such as voltage regulators. Since the PV power

integration continuously increases, the distribution grid owner needs a way to improve the ability of the network to absorb PV generation. The PVAC improvement should be considered from the long-term perspective.

Optimal voltage regulator (VR) planning is an effective approach to enhance the PVAC in the distribution grid since VR can regulate voltage magnitude. The VR is known as the step voltage regulator and includes an autotransformer. During the voltage regulation process, the voltage magnitude variation can be obtained by changing the number of turns (tap changers) in the series winding of the autotransformer. VR has many advantages, especially fast and efficient operational metrics [25]. To some extent, VR can address the voltage fluctuation problem caused by renewable energy and thus has an influence on PVAC enhancement by alleviating overvoltage violations. However, some classical studies [26]–[29] related to VR planning overlook the potential of VR planning for improving the PVAC. Therefore, this paper endeavors to improve the PVAC via optimal VR planning in distribution grids.

In this paper, a novel bi-level optimization based VR planning model is proposed for incentive-based PV energy integration maximization. The proposed optimization model is formulated as a Benders decomposition based bi-level problem. In the upper-level problem, VR planning decisions and PVAC are determined via the mixed integer linear programming. Then in the lower-level problem, the feasibility of first-level results is checked by critical network constraints (e.g. voltage magnitude constraints and line capacity constraints) under uncertainties including load and PV generation. To represent these uncertainties, operational scenarios are generated and selected by the Gaussian copula theory and a well-studied backward-reduction algorithm, respectively. The modified 33-node distribution grid is utilized to verify the effectiveness of the proposed model and solution method. The results demonstrate that hourly PVAC can be significantly enhanced with optimal VR planning. The major contributions of this paper are summarized as follows:

- 1) The main contribution of this work is the investigation of the potential benefits from optimal VR planning, as an option to improve the PV energy integration of distribution grids. This work has a practical significance by considering the widespread application of VRs in power systems.
- 2) Instead of using conventional time-consuming simulation-based methods to evaluate the hourly amount of PV energy that can be integrated into the distribution grids, this paper introduces the concept of PVAC, which is modeled by the optimization context and incorporated into the objective function.
- 3) To maintain the safety and reliability of the distribution grid operation, two criteria are introduced, i.e., voltage variation and line capacity. Then the stochastic programming-based feasibility check model is proposed to guarantee the security of distribution grids for any considered operational scenarios.

The remainder of this paper is organized as follows: Section II provides the system modeling. Section III introduces the problem formulation and solution method. Case studies

are demonstrated in Section IV. Section V presents concluding remarks.

II. SYSTEM MODELING

A. Uncertainty Consideration

During the decision-making process of VR planning, uncertainties arising from load and PV generation should be duly considered. In this paper, these two uncertainties are described in the form of operational scenarios, in which the load can be fitted by the normal distribution [30] in the long term, while the PV generation is highly related to the solar irradiance, which is usually modeled by a Beta distribution [31]. In obtaining distribution information, the Gaussian copula theory [32] is employed to generate standard Gaussian random variables, which can be transformed into operational scenarios by the inverse transform method [33].

Generally, the obtained solution becomes robust with more operational scenarios considered. However, solving optimization problems with numerous operational scenarios may result in a huge computation burden [34]. In this regard, representative scenarios should be distinguished before the optimization process, to guarantee the robustness of the solution and ensure acceptable computation time. Here, a Kantorovich Distance (KD) [35] based scenario reduction method is adopted for scenario reduction since this algorithm can generate weights of each selected scenario, and distinguishing the importance of each scenario. KD can be calculated according to the following equation:

$$d_{\text{KD}}(\chi^{(m)}, \chi^{(n)}) = \sqrt{\left(\sum_{\lambda}^{N_{\lambda}} (\nu_{\lambda}^{(m)} - \nu_{\lambda}^{(n)})^2 \right)} \quad (1)$$

where $d_{\text{KD}}(\chi^{(m)}, \chi^{(n)})$ is the KD between two scenarios $\chi^{(m)}$ and $\chi^{(n)}$, N_{λ} is the number of stages in the optimization problem, λ is the stage, ν_{λ} is the vector value of the scenario at stage λ , m and n are the scenario numbers.

Algorithm 1 describes the implementation procedure of the KD based scenario reduction method. Finally, each representative scenario $w \in \mathcal{W}$ consists of three vectors, denoting active load, reactive load and PV output factor, given as, $w = \{p_{jtw}, q_{jtw}, \mu_{jtw}^{\text{PV}}\}$.

Algorithm 1: KD based Scenario Reduction Method

```

1 Initialize
2   Calculate the KD of each scenario pair via (1)
3   Build the KD matrix
4   Repeat
5     Randomly evaluate the scenario  $\chi^m$  via
        $\min\{d_{\text{KD}}(\chi^m, \chi^n)\}$ 
6     Eliminate one scenario via
        $\min\{\min\{d_{\text{KD}}(\chi^m, \chi^n)\} \times P_m\}$ 
7     Build the new KD matrix
8     Add the probability of the eliminated scenario
       to the probability of the closest one
9   Until stopping criterion has been met
10 End

```

B. Piecewise Linearized DistFlow Model

In this paper, the DistFlow model [36] is utilized to describe the complex power flows at the node j in a distribution network, given as follows:

$$P_{jtw} = \sum_{i \in \phi(j)} P_{itw} + \sum_{i \in \phi(j)} r_{ij} \frac{P_{itw}^2 + Q_{itw}^2}{V_{itw}^2} + p_{jtw}, \quad \forall j \in J, \forall t \in T, \forall w \in W \quad (2)$$

$$Q_{jtw} = \sum_{i \in \phi(j)} Q_{itw} + \sum_{i \in \phi(j)} x_{ij} \frac{P_{itw}^2 + Q_{itw}^2}{V_{itw}^2} + q_{jtw}, \quad \forall j \in J, \forall t \in T, \forall w \in W \quad (3)$$

$$V_{jtw} = V_{itw} + \frac{r_{ij}P_{itw} + x_{ij}Q_{itw}}{V_0}, \quad \forall j \in J, i \in \phi(j), \quad \forall t \in T, \forall w \in W \quad (4)$$

$$V_{jtw} = V^{\text{Sub}}, \quad j = 1, \forall t \in T, \forall w \in W \quad (5)$$

where (1) and (2) describe the active and reactive power flow balance, respectively. (3) denotes the voltage along the distribution line ij .

To deal with nonlinearity caused by quadratic terms, such as P_{itw}^2 and Q_{itw}^2 , we employ the piecewise linearized DistFlow equations [37] which linearizes these two quadratic terms to more accurately calculate the apparent power. The following piecewise linearized DistFlow equations characterize the set of power flow and PV output:

$$P_{jtw} = \sum_{i \in \phi(j)} P_{itw} + \sum_{i \in \phi(j)} r_{ij} \frac{P_{itw}^{\text{QT}} + Q_{itw}^{\text{QT}}}{V_0^2} + p_{jtw} - \sum_j P_{jtw}^{\text{PV}}, \quad \forall j \in J, \forall t \in T, \forall w \in W \quad (6)$$

$$Q_{jtw} = \sum_{i \in \phi(j)} Q_{itw} + \sum_{i \in \phi(j)} x_{ij} \frac{P_{itw}^{\text{QT}} + Q_{itw}^{\text{QT}}}{V_0^2} + q_{jtw} + \sum_j Q_{jtw}^{\text{PV}}, \quad \forall j \in J, \forall t \in T, \forall w \in W \quad (7)$$

$$V_{jtw} = V_{itw} + \frac{r_{ij}P_{itw} + x_{ij}Q_{itw}}{V_0}, \quad \forall j \in J, i \in \phi(j), \forall t \in T, \forall w \in W \quad (8)$$

$$V_{jtw} = V^{\text{Sub}}, \quad j = 1, \forall t \in T, \forall w \in W \quad (9)$$

where (6)–(8) are derived from (1)–(3). The quadratic terms P_{jtw}^{QT} and Q_{jtw}^{QT} are employed to estimate P_{jtw}^2 and Q_{jtw}^2 . By using the piecewise linearization approximation (PLA) approach [37], the quadratic terms P_{jtw}^{QT} and Q_{jtw}^{QT} can be estimated by the following two equations:

$$P_{jtw}^{\text{QT}} \geq M_{\alpha jtw}^{\text{AP}} P_{jtw} + N_{\alpha jtw}^{\text{AP}}, \quad \forall \alpha \in \Omega^{\text{AP}}, \forall j \in J, \forall t \in T, \forall w \in W \quad (10)$$

$$Q_{jtw}^{\text{QT}} \geq M_{\alpha jtw}^{\text{RP}} Q_{jtw} + N_{\alpha jtw}^{\text{RP}}, \quad \forall \alpha \in \Omega^{\text{RP}}, \forall j \in J, \forall t \in T, \forall w \in W \quad (11)$$

where $M_{\alpha jtw}^{\text{AP}}$, $M_{\alpha jtw}^{\text{RP}}$, $N_{\alpha jtw}^{\text{AP}}$ and $N_{\alpha jtw}^{\text{RP}}$ are the constant coefficient of the PLA approach.

In addition, we assume PV systems can provide reactive power support to the distribution network and the range of

reactive power output is given as follows:

$$\underline{Q}_{jtw}^{PV} \leq Q_{jtw}^{PV} \leq \overline{Q}_{jtw}^{PV}, \quad j \in J, \forall t \in T, \forall w \in W \quad (12)$$

where $\underline{Q}_{jtw}^{PV} = -\overline{Q}_{jtw}^{PV}$ and $\overline{Q}_{jtw}^{PV} = P_{jtw}^{PV} \cdot \tan \theta_{pv}$.

C. Voltage Regulation Installation Model

Figure 1 depicts one distribution branch diagram with a VR. For simplification, we assume that each VR has a regulator range of $rr\%$ and the VR tap position is considered as a continuous variable [38]. The mathematical VR planning and operational model can be formulated as follows:

$$\tilde{V}_{jtw} = V_{itw} + \frac{r_{ij}P_{itw} + x_{ij}Q_{itw}}{V_0}, \quad \forall j \in J, i \in \phi(j), \forall t \in T, \forall w \in W \quad (13)$$

$$(1 - rr\%) \tilde{V}_{jtw} \leq V_{jtw} \leq (1 + rr\%) \tilde{V}_{jtw}, \quad \forall j \in J, \forall t \in T, \forall w \in W \quad (14)$$

$$|V_{jtw} - \tilde{V}_{jtw}| \leq (V^{\text{Max}} - V^{\text{Min}}) u_j^{\text{VR}}, \quad \forall j \in J, \forall t \in T, \forall w \in W \quad (15)$$

where (13) describes the voltage transit along the distribution branch between the node i and the VR installation point. (14) and (15) describe the relationship of the voltage magnitude between the VR installation point and the node j . Note that if $u_j^{\text{VR}} = 0$, (without VR installation), then $V_{jtw} = \tilde{V}_{jtw}$, otherwise, V_{jtw} varies in $[(1 - rr\%), (1 + rr\%)] \tilde{V}_{jtw}$.

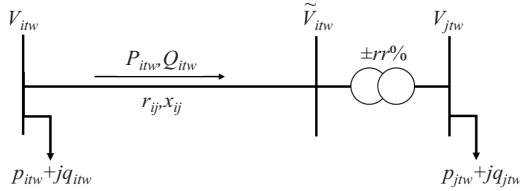


Fig. 1. One branch diagram with a VR installed.

III. PROBLEM FORMULATION AND SOLUTION

In this section, we first formulate the bi-level optimization based VR planning model to maximize the hourly PVAC of the distribution system. Specifically, in the upper-level problem, optimal VR planning decisions and hourly PV hosting capacity decisions can be made without consideration of network constraints. The lower-level problem is based on the feasibility checking model, in which critical network constraints with the upper-level results, e.g., voltage magnitude constraints and line capacity constraints, are ensured for the security of the system operation. Then, a solution method is proposed

to iteratively solve the upper-level problem and lower-level problem. Figure 2 depicts the proposed optimization based bi-level framework.

A. Upper-level Problem Formulation

The upper-level problem is based on mixed integer linear programming (MILP), aiming to find the optimal VR planning decisions and hourly PV hosting capacity. The detailed upper-level problem formulation is given as follows,

$$\text{Min} \sum_{j \in J} (\kappa c_{inv}^{\text{VR}} + c_{o\&m}^{\text{VR}}) u_j^{\text{VR}} - \sum_{w \in W} p_w \sum_{t \in T} \sum_{j \in J} c^{\text{PV}} \mu_{tw}^{\text{PV}} Z_j^{\text{PV}} \quad (16)$$

$$\text{s.t.} \sum_{j \in J} c_{inv}^{\text{VR}} u_j^{\text{VR}} \leq C^{\text{VR}} \quad (17)$$

$$u_j^{\text{VR}} \in [0, 1], u_j^{\text{VR}} \in R, \quad j \in J \quad (18)$$

$$E_j^{\text{PV}} \geq 0, \quad j \in J \quad (19)$$

$$u_j^{\text{PV}} \in [0, 1], u_j^{\text{PV}} \in R, \quad j \in J \quad (20)$$

$$0 \leq Z_j^{\text{PV}} \leq u_j^{\text{PV}} B^{\text{M}}, \quad \forall j \in J \quad (21)$$

$$Z_j^{\text{PV}} \leq E_j^{\text{PV}}, \quad \forall j \in J \quad (22)$$

$$Z_j^{\text{PV}} + B^{\text{M}} - E_j^{\text{PV}} - u_j^{\text{PV}} B^{\text{M}} \geq 0, \quad \forall j \in J \quad (23)$$

where (16) describes the objective function of the upper-level problem, which is to minimize the VR planning cost (the first term) and meanwhile maximize the revenue of PV energy integration in the first term. $\kappa = \frac{r(1+r)^y}{365[(1+r)^y - 1]}$ is the daily recovery factor, which is introduced here to transform the VR investment cost c_{inv}^{VR} into the daily value. r and y represent the interest rate and planning horizon, respectively. $c_{o\&m}^{\text{VR}}$ denotes the daily VR operating & maintenance cost. u_j^{VR} represents the binary decision variable for VR installation status, i.e., installation ($u_j^{\text{VR}} = 1$) or not ($u_j^{\text{VR}} = 0$). In the second term, p_w is the probability of the uncertainty scenario. c^{PV} denotes the subsidy for PV generation integration. Note that the subsidy is decided by relative policies, but in this study, we assume that it can be increased by the local distribution grid operator to simulate the improvement of PV energy penetration. PV output factor $\mu_{tw}^{\text{PV}} \in [0, 1]$ is used to capture the PV generations. An auxiliary continuous variable Z_j^{PV} is introduced to replace the bilinear term $u_j^{\text{PV}} E_j^{\text{PV}}$. (17) considers the practical total VR capital cost limit and (18) defines the binary variable u_j^{VR} . The continuous variable E_j^{PV} in (19) denotes the size of PV generation connected to the node j . In (20), the binary variable u_j^{PV} represents whether the PV generation is connected to the node j . The Big M method [39] is used in (21), (22) to linearize the nonlinear term $u_j^{\text{PV}} E_j^{\text{PV}}$, which is replaced by an auxiliary continuous variable Z_j^{PV} . Note that B^{M} is a positive constant, and is large enough.

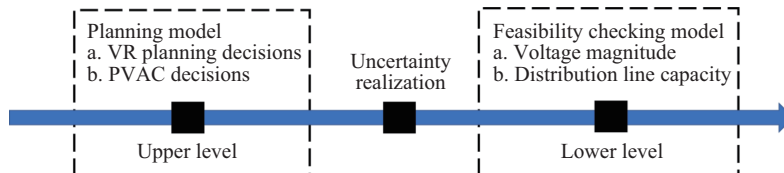


Fig. 2. Bi-level optimization based framework.

In the following subsection, we will give the formulation of lower-level problem formulation.

B. Lower-level Problem Formulation

The proposed lower-level problem can be formulated to a feasibility checking model, given as follows,

$$\text{Min} \sum_{j \in J} c^{\text{Penalty}} \left(s_{jtw}^{V, \text{LB}} + s_{jtw}^{V, \text{UB}} + s_{jtw}^{\text{PQ}} \right) \quad (24)$$

s.t. (6)–(12), (13)–(15)

$$V_{jtw} + s_{jtw}^{V, \text{LB}} \geq V, \quad \forall j \in J, \forall t \in T, \forall w \in W \quad (25)$$

$$V_{jtw} - s_{jtw}^{V, \text{UB}} \leq \bar{V}, \quad \forall j \in J, \forall t \in T, \forall w \in W \quad (26)$$

$$P_{jtw}^{\text{QT}} + Q_{jtw}^{\text{QT}} - s_{jtw}^{\text{PQ}} \leq LC_{ij}^2, \quad \forall j \in J \setminus 1, \forall t \in T, \forall w \in W \quad (27)$$

$$P_{jtw}^{\text{QT}} + Q_{jtw}^{\text{QT}} - s_{jtw}^{\text{PQ}} \leq SC^2, \quad j = 1, \forall t \in T, \forall w \in W \quad (28)$$

$$s_{jtw}^{V, \text{LB}}, s_{jtw}^{V, \text{UB}}, s_{jtw}^{\text{PQ}} \in R^+, \quad \forall j \in J, \forall t \in T, \forall w \in W \quad (29)$$

where the optimal objective (24) in the lower-level problem should be zero because of the enforced penalty cost. Where constraints (6)–(12) and (13)–(15) describe the power flow constraints and the VR model, respectively. (25) and (26) show relaxed voltage constraints. The limits of relaxed distribution branch capacity as well as the substation capacity are described in (27) and (28), respectively.

C. Iterative Solution Procedure

Generally, the upper-level problem (16)–(23) and lower-level problem (24)–(29) can be combined to form a conventional two-stage stochastic programming problem, which can be solved with commercial solvers, such as CPLEX [40] and GURIBO [41]. However, to guarantee the robustness of the solution, a reasonable number of operational scenarios should be taken into account during the decision-making process. This can cause a huge computation burden since numerous variables and constraints are involved in the stochastic problem. To deal with the aforementioned issues, an efficient solution approach is introduced in this section. The upper-level problem ignores the network constraints, so the result of objective (16) in the upper-level problem can be regarded as the lower bound of the combined two-stage stochastic programming problem. Given the upper-level results, objective (24) in the lower-level problem can be used to obtain the upper bound. In Algorithm 2, Step 4 and Step 6 are executed iteratively to update the lower bound $Z^{\text{Lower}(v)}$ and upper bound $Z^{\text{Upper}(v)}$. It should be noted that an additional constraint is added to link the upper-level problem and lower-level problem. In this constraint, dual variables $\lambda_{jtw}^{\text{PV}(v)}$ and $\lambda_{jtw}^{\text{VR}(v)}$ are included to provide the sensitivities of the upper-level variables $Z_j^{\text{PV}(v)}$ and $u_j^{\text{VR}(v)}$, respectively.

IV. CASE STUDIES

The performance of the proposed method is validated on the IEEE 33-node distribution grid (see Fig. 3). The parameters details of this test system can be referred to [42]. In this paper, we consider a five-year planning horizon. One hundred

Algorithm 2: Iterative Solution Procedure

1 Initialization.

Convergence controller $\varepsilon = 0.01$

Iteration counter $v = 0$

2 Repeat

3 $v \leftarrow v + 1$

4 Solve the upper-level problem as follows

$$Z^{\text{Lower}(v)} := \text{Min} \gamma^{(v)} + \sum_{j \in J} (\kappa c_{inv}^{\text{VR}} + c_m^{\text{VR}}) u_j^{\text{VR}(v)} - \sum_{w \in W} p_w \sum_{t \in T} \sum_{j \in J} c^{\text{PV}} \mu_{tw}^{\text{PV}} Z_j^{\text{PV}(v)}$$

s.t. (17)–(23)

$$\gamma^{(v)} \geq \sum_{j \in J} \sum_{w \in W} \rho_w \sum_{t \in T} \lambda_{jtw}^{\text{VR}(v)} \left(u_j^{\text{VR}(v)} - u_j^{\text{VR}(\tau)} \right) + \sum_{j \in J} \sum_{w \in W} \rho_w \sum_{t \in T} \lambda_{jtw}^{\text{PV}(v)} \left(Z_j^{\text{PV}(v)} - Z_j^{\text{PV}(\tau)} \right) + \sum_{w \in W} \rho_w \sum_{t \in T} Z_{tw}^{\text{Sub}(k)} \quad \tau = 1, 2, \dots, v-1$$

5 Update $Z_j^{\text{PV}(v)}$ and $u_j^{\text{VR}(v)}$ and $Z^{\text{Lower}(v)}$

6 Solve the lower-level problem as follow

$$Z_{tw}^{\text{Sub}(v)} := \text{Min} \sum_{j \in J} c^{\text{Penalty}} \left(s_{jtw}^{V, \text{LB}} + s_{jtw}^{V, \text{UB}} + s_{jtw}^{\text{PQ}} \right) \text{ s.t. (6)–(15), (25)–(29)} \\ Z_j^{\text{PV}(v)} = Z_j^{\text{PV}*} : \lambda_{jtw}^{\text{PV}(v)}, \forall j \in J, \forall t \in T, \forall w \in W \\ u_j^{\text{VR}(v)} = u_j^{\text{VR}*} : \lambda_{jtw}^{\text{VR}(v)}, \forall j \in J, \forall t \in T, \forall w \in W$$

7 Output $Z_{tw}^{\text{Sub}(v)}$, $\lambda_{jtw}^{\text{PV}(v)}$ and $\lambda_{jtw}^{\text{VR}(v)}$

8 Calculate $Z^{\text{Upper}(v)}$ via the following equation

$$Z^{\text{Upper}(v)} = \sum_{w \in W} p_w \sum_{t \in T} Z_{tw}^{\text{Sub}(v)} + \sum_{j \in J} (\kappa c_{inv}^{\text{VR}} + c_m^{\text{VR}}) u_j^{\text{VR}(v)} - \sum_{w \in W} p_w \sum_{t \in T} \sum_{j \in J} c^{\text{PV}} \mu_{tw}^{\text{PV}} Z_j^{\text{PV}(v)}$$

9 Until $|Z^{\text{Upper}(v)} - Z^{\text{Lower}(v)}| \leq \varepsilon$

10 Output optimal results, $Z_j^{\text{PV}*}$, $u_j^{\text{VR}*}$

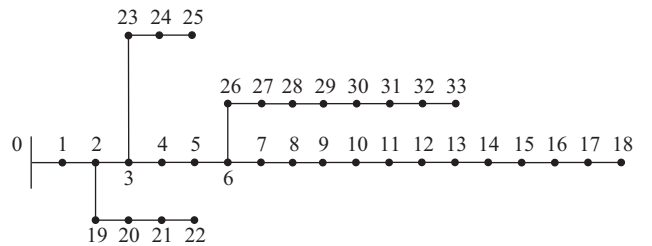


Fig. 3. IEEE 33-node test distribution grid.

representative operation samples with different weights are selected, which includes ten load demand scenarios (see Fig. 4) and ten PV output scenarios (see Fig. 5). Table I summarizes the parameters in this test case including VR investment cost, VR operating and maintenance cost, subsidy for PV generation integration, penalty coefficient for violations, base

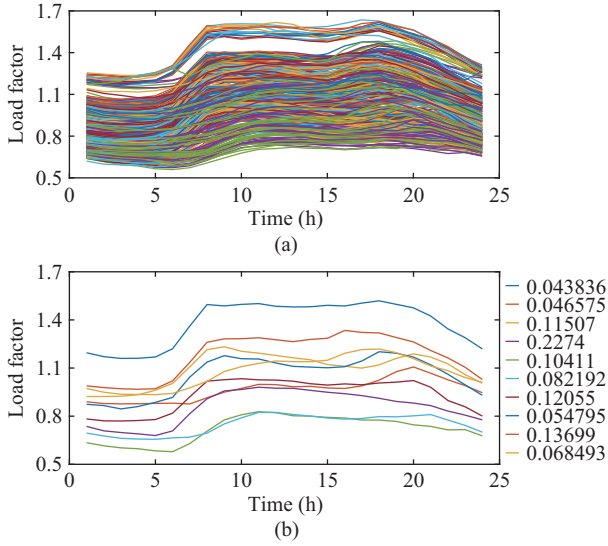


Fig. 4. Load scenarios (a) before and (b) after scenario reduction.

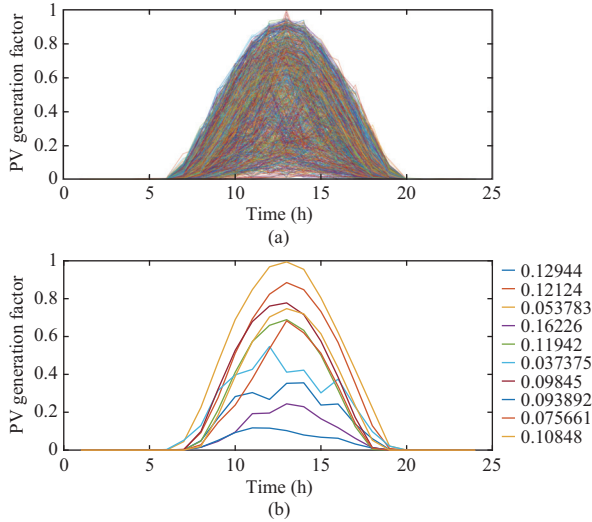


Fig. 5. PV generation scenarios (a) before and (b) after scenario reduction.

TABLE I
RELATED PARAMETERS IN TEST CASE

| Parameter | Parameter value |
|---|---------------------|
| VR investment cost c_{inv}^{VR} | 5,000 \$ [29] |
| VR operating and maintenance cost $c_{o\&m}^{VR}$ | 5 \$/day [43] |
| Subsidy for PV generation integration c^{PV} | 0.39 \$/(kW·h) [44] |
| Penalty coefficient for violations $c^{Penalty}$ | 100,000 \$/p.u. |
| Base energy value | 1 MVA |
| Base voltage value | 12.66 kV |

energy value, and base voltage value.

A. Performance of Computation Efficiency

Figure 6 depicts the evolution of the proposed iterative solution method. In the 37th iteration, this algorithm converges where the gap between the upper bound and the lower bound is smaller than the predefined tolerance. To demonstrate the computational efficiency of our proposed approach, a comparison between these two solution methods is conducted:

1) directly using the commercial solver (e.g. GUROBI [41]);
2) proposed method. As shown in Table II, both solution methods can be used to solve the proposed problem with low considered scenario numbers (e.g. 1, 9, 25) while our proposed method shows a clear advantage over the first method, and this advantage is widened as the scenario numbers increase. With high scenario numbers (e.g. 64, 100), a huge computation burden may be involved so the commercial solver cannot handle the original problem. By contrast, our proposed method can solve the same problem with acceptable computation time.

B. Performance of Optimal VR Planning

In this subsection, we demonstrate the performance of the optimal VR planning. It can be seen from Table III that the value of PVAC is 0.0444 p.u and Table IV shows the corresponding VR planning decisions. In order to demonstrate the performance of VR planning on the PVAC enhancement, Case 1 (the base case without VR installation) and Case 2 (the case with VR installation) are compared as shown in Fig. 7. We can observe from these figures that the PVAC is significantly improved after VR installation.

Figure 8 depicts two voltage profiles at 12:00 pm under the expected scenario in which loads and PV generations are

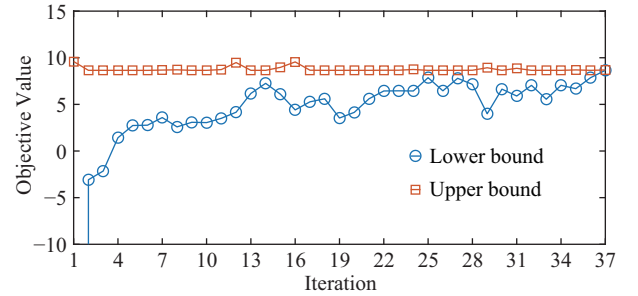


Fig. 6. Evolution of the decomposition solution algorithm.

TABLE II
COMPARISONS OF COMPUTATION TIME

| Scenario number | Computation time (min) | |
|-----------------|------------------------|-----------------|
| | GUROBI solver | Proposed method |
| 1 (1 × 1) | 0.22 | 0.19 |
| 9 (3 × 3) | 27.36 | 4.57 |
| 25 (5 × 5) | 132.27 | 18.56 |
| 64 (8 × 8) | N.A. | 53.33 |
| 100 (10 × 10) | N.A. | 105.28 |

TABLE III
RESULT OF THE PVAC IN THE 33-NODE TEST SYSTEM

| Locations (nodes) | PVAC Value (p.u.) |
|-------------------|-------------------|
| 5 | 0.0187 |
| 10 | 0.0028 |
| 16 | 0.0042 |
| 21 | 0.0044 |
| 23 | 0.0123 |
| 27 | 0.0010 |
| 32 | 0.0010 |

TABLE IV
VR PLANNING RESULT IN THE 33-NODE TEST SYSTEM

| Locations (nodes) | 5, 6, 22, 25, 26, 28, 30, 31 |
|-------------------|------------------------------|
|-------------------|------------------------------|

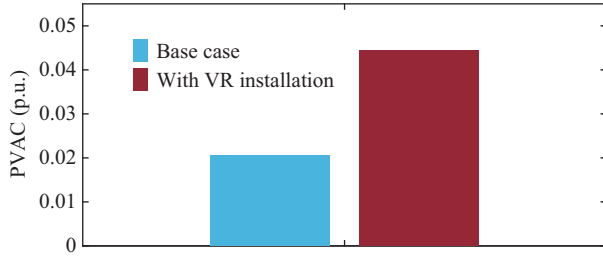


Fig. 7. Comparison of PVAC with and without VR installation.

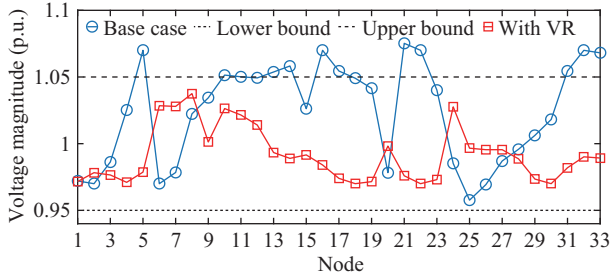


Fig. 8. Comparison of voltage magnitude.

their mean values: (1) voltage profile of the case with PV generators but without VR installation, and (2) voltage profile of the case with both PV integration and VR installation, as the results show in Tables III and IV. As seen in this figure, the voltage magnitudes on some nodes, i.e., nodes 5, 14, 16, 17, 21, 22, 31, 32, and 33 exceed the upper bound (1.05 p.u.) in the first case due to the lack of the voltage adjustment of the VR. However, the overvoltage violations caused by high PV penetration can be avoided after optimal VR planning, as shown in the second case.

Figures 9 and 10 show the comparison results for the apparent power of the 33-node test system in two representative scenarios, i.e. scenario 17 and scenario 55. Note that the apparent power S_{jtw} can be calculated by using the following equation,

$$S_{jtw} = \sqrt{P_{jtw}^{QT} + Q_{jtw}^{QT}}, \forall j \in J \setminus 1, \forall t \in T, \forall w \in W \quad (30)$$

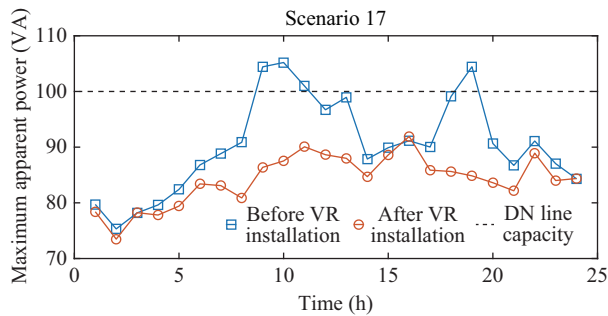


Fig. 9. Comparison of maximum apparent power in scenario 17.

As shown in Figs. 9 and 10, the line overload can be observed before VR installation. In comparison, the apparent power flow is maintained within its desired range after VR installation. According to these comparisons, we can conclude

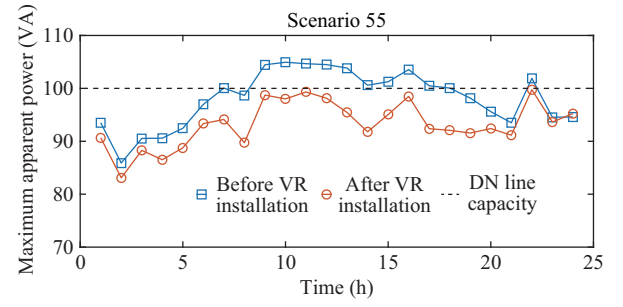


Fig. 10. Comparison of maximum apparent power in scenario 55.

that the optimal VR allocation can not only avoid overvoltage occurrence, but also ensure the safe operation of the lines.

C. Comparison with Deterministic Model

In this subsection, the deterministic VR planning model is employed as a benchmark. The deterministic model only uses one operational scenario as its input, in which the PV output and load demand are replaced by their expected values. By solving the deterministic VR planning problem, we can obtain the optimal VR installation sites: nodes 15, 16, 19, 21, 23, and 27. Together with the deterministic VR planning decisions, the PVAC values are 0.0106, 0.0001, 0.0007, 0.0064, 0.0021, 0.0036 and 0.0079 p.u. for nodes 5, 10, 16, 21, 23, 27 and 32, respectively.

To compare the performance of the deterministic model and the stochastic model, the critical operational scenario corresponding to the maximum PV output factor with the minimum load demand level is utilized. Fig. 11(a) and Fig. 11(b) depict the voltage profiles obtained by the deterministic model and stochastic model under this critical scenario, respectively. From these two figures, the overvoltage violation can be seen in Fig. 11(a) while this violation cannot be observed in Fig. 11(b).

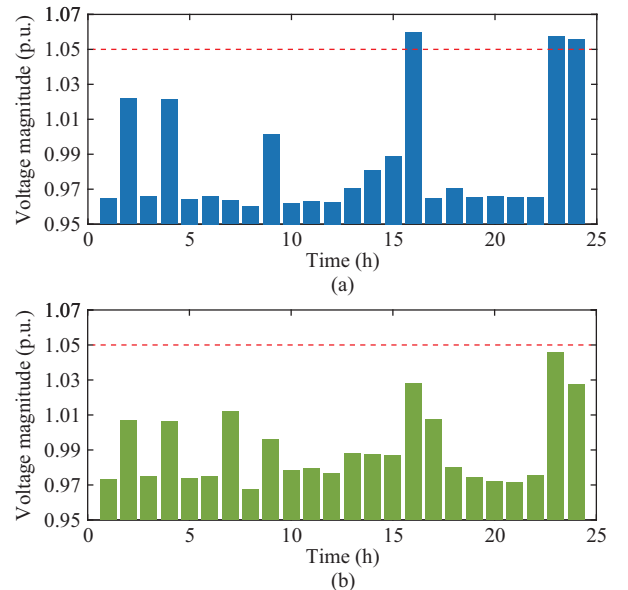


Fig. 11. Comparison results of (a) the deterministic model and (b) the stochastic model.

D. Tradeoff curve between PVAC and VR planning cost

Figure 12 is plotted to describe the relationship between the PVAC and VR planning cost. This figure shows that the PVAC increases gradually before the VR planning cost reaches about \$450,000. Then the increasing rate is marginal, which means that the PVAC improvement is insensitive to the additional VR planning cost. The reason is that there is a threshold determined by the loadability of the power grid [45], which means there are overload issues on distribution grid lines, including overvoltage issues on the distribution grid nodes that may occur under the larger PV integration. When the PVAC improvement is too little to be acceptable by microgrid owners, network expansion is recommended.

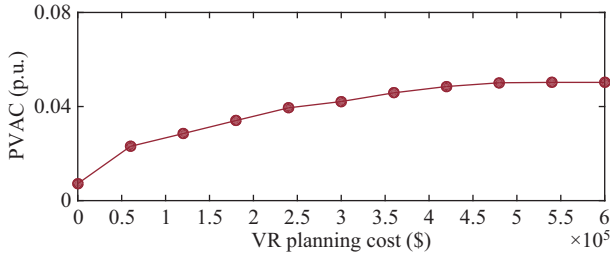


Fig. 12. Tradeoff curve between the PVAC and VR planning cost.

E. Impact of VR Installation Number on PVAC

This subsection presents a sensitivity analysis examining the impact of the VR installation number on the PVAC under the expected operational scenario. As shown in Fig. 13, PVAC increases almost linearly with respect to the VR installation number. However, after an installation of eight VRs, the increasing rate of PVAC becomes marginal. Finally, the value of PVAC is fixed when twelve or more VRs are placed. The reason is that the line capacity limits the threshold of the PVAC, which may be further improved after network expansion.

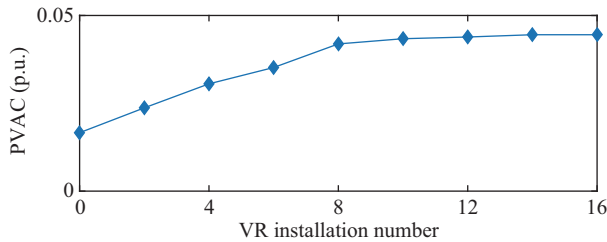


Fig. 13. Impact of VR installation number on the PVAC.

V. CONCLUSION

This paper presents a novel bi-level Benders decomposition based stochastic VR planning model for distribution grids considering PV energy integration maximization. As a widely-used device in power systems, optimal VR planning can be regarded as a feasible option to improve the PV energy integration by regulating voltage magnitudes. To describe the dynamic amount of PV energy that can be integrated into the power system, the concept of PVAC is introduced and modeled

with optimization. Uncertainties of PV generations and loads are duly considered during the planning stage, which are represented in the form of representative operational scenarios. Facing the challenge with numerous scenarios and time coupling constraints, a well-studied decomposition algorithm is employed as the solution method. Based on the IEEE 33-node distribution system, the benefits of optimal VR planning for PV energy integration improvement are illustrated in the case studies. The proposed model provides a reference for distribution system planners. The main conclusions are summarized as: 1) From the case studies, the PV energy integration can be significantly improved by using the proposed VR planning model; 2) Reliable Distribution grid operations can be ensured by the VR since it can regulate nodal voltage magnitudes and relieves overload; 3) The loadability of the distribution grid generates a threshold beyond which the PVAC is insensitive to the additional VR installation. In future studies, it would be interesting to coordinately analyze the effect of planning and operations of advanced voltage regulation devices to improve PV energy integration. In addition, the simultaneous improvement of various renewable energy integrations, including wind generators via our proposed model could be investigated.

REFERENCES

- [1] X. Liu, Y. Liu, J. Liu, Y. Xiang, and X. Yuan, "Optimal planning of AC-DC hybrid transmission and distributed energy resource system: Review and prospects," *CSEE Journal of Power Energy Systems*, vol. 5, no. 3, pp. 409–422, 2019.
- [2] V. Telukunta, J. Pradhan, A. Agrawal, M. Singh, and S. G. Srivani, "Protection challenges under bulk penetration of renewable energy resources in power systems: A review," *CSEE journal of power energy systems*, vol. 3, no. 4, pp. 365–379, 2017.
- [3] S. Wang, "Current status of PV in China and its future forecast," *CSEE Journal of Power and Energy Systems*, vol. 6, no. 1, pp. 72–82, 2020.
- [4] X. Deng and T. Lv, "Power system planning with increasing variable renewable energy: A review of optimization models," *Journal of Cleaner Production*, vol. 246, pp. 118962, 2020.
- [5] X. Chen, K.-C. Leung, and A. Y. Lam, "Power Output Smoothing for Renewable Energy System: Planning, Algorithms, and Analysis," *IEEE Systems Journal*, vol. 14, no. 1, pp. 1034–1045, 2020.
- [6] G. P. Baker, M. C. Jensen, and K. J. Murphy, "Compensation and incentives: Practice vs. theory," *The Journal of Finance*, vol. 43, no. 3, pp. 593–616, 1988.
- [7] C. S. Lai, G. Locatelli, A. Pimm, Y. Tao, X. Li, and L. L. Lai, "A financial model for lithium-ion storage in a photovoltaic and biogas energy system," *Applied Energy*, vol. 251, pp. 113179, 2019.
- [8] Y. Jia, Z. Xu, L. L. Lai, and K. P. Wong, "Risk-based power system security analysis considering cascading outages," *IEEE Transactions on Industrial Informatics*, vol. 12, no. 2, pp. 872–882, 2016.
- [9] Y. Guo, L. Tong, W. Wu, B. Zhang, and H. Sun, "Coordinated multi-area economic dispatch via critical region projection," *IEEE Transactions on Power Systems*, vol. 32, no. 5, pp. 3736–3746, 2017.
- [10] F. Ding and B. Mather, "On Distributed PV Hosting Capacity Estimation, Sensitivity Study, and Improvement," *IEEE Transactions on Sustainable Energy*, vol. 8, no. 3, pp. 1010–1020, 2017.
- [11] S. Shamshirband, T. Rabczuk, and K.-W. Chau, "A Survey of Deep Learning Techniques: Application in Wind and Solar Energy Resources," *IEEE Access*, vol. 7, pp. 164650–164666, 2019.
- [12] S. Samadianfard, A. Majnooni-Heris, S. N. Qasem, O. Kisi, S. Shamshirband, and K.-w. Chau, "Daily global solar radiation modeling using data-driven techniques and empirical equations in a semi-arid climate," *Engineering Applications of Computational Fluid Mechanics*, vol. 13, no. 1, pp. 142–157, 2019.
- [13] U. Beyaztas, S. Q. Salih, K.-W. Chau, N. Al-Ansari, and Z. M. Yaseen, "Construction of functional data analysis modeling strategy for global solar radiation prediction: application of cross-station paradigm," *Engineering Applications of Computational Fluid Mechanics*, vol. 13, no. 1, pp. 1165–1181, 2019.

- [14] F. Hosseini-Fashami, A. Motevali, A. Nabavi-Pelesaraei, S. J. Hashemi, and K.-w. Chau, "Energy-Life cycle assessment on applying solar technologies for greenhouse strawberry production," *Renewable and Sustainable Energy Reviews*, vol. 116, pp. 109411, 2019.
- [15] A. Baghban, A. Jalali, M. Shafiee, M. H. Ahmadi, and K.-w. Chau, "Developing an ANFIS-based swarm concept model for estimating the relative viscosity of nanofluids," *Engineering Applications of Computational Fluid Mechanics*, vol. 13, no. 1, pp. 26–39, 2019.
- [16] B. Najafi, S. Faizollahzadeh Ardabili, S. Shamshirband, K.-w. Chau, and T. Rabczuk, "Application of ANNs, ANFIS and RSM to estimating and optimizing the parameters that affect the yield and cost of biodiesel production," *Engineering Applications of Computational Fluid Mechanics*, vol. 12, no. 1, pp. 611–624, 2018.
- [17] A. Rabiee and S. M. Mohseni-Bonab, "Maximizing hosting capacity of renewable energy sources in distribution networks: A multi-objective and scenario-based approach," *Energy*, vol. 120, pp. 417–430, 2017.
- [18] S. Hashemi, J. stergaard, T. Degner, R. Brandl, and W. Heckmann, "Efficient control of active transformers for increasing the pv hosting capacity of lv grids," *IEEE Transactions on Industrial Informatics*, vol. 13, no. 1, pp. 270–277, 2017.
- [19] Y. Jia, X. Lyu, P. Xie, Z. Xu and M. Chen, "A Novel Retrospect-inspired Regime for Microgrid Real-time Energy Scheduling with Heterogeneous Sources," *IEEE Transactions on Smart Grid*, doi: 10.1109/TSG.2020.2999383.
- [20] X. Xu, Y. Jia, Y. Xu, Z. Xu, S. Chai, and C. S. Lai, "A Multi-agent Reinforcement Learning based Data-driven Method for Home Energy Management," *IEEE Transactions on Smart Grid*, 2020.
- [21] J. Youwei, L. Xue, C. S. Lai, X. Zhao, and C. Minghua, "A retroactive approach to microgrid real-time scheduling in quest of perfect dispatch solution," *Journal of Modern Power Systems and Clean Energy*, vol. 7, no. 6, pp. 1608–1618, 2019.
- [22] A. Soroudi, A. Rabiee, and A. Keane, "Distribution networks' energy losses versus hosting capacity of wind power in the presence of demand flexibility," *Renewable Energy*, vol. 102, pp. 316–325, 2017.
- [23] S. Hashemi and J. Ostergaard, "Efficient control of energy storage for increasing the PV hosting capacity of LV grids," *IEEE Transactions on Smart Grid*, 2016.
- [24] S. Wang, S. Chen, L. Ge, and L. Wu, "Distributed generation hosting capacity evaluation for distribution systems considering the robust optimal operation of oltc and svc," *IEEE Transactions on Sustainable Energy*, vol. 7, no. 3, pp. 1111–1123, 2016.
- [25] S. Nakashima, "Voltage regulator," ed: Google Patents, 2019.
- [26] M. Attar, O. Homaei, H. Falaghi, and P. Siano, "A novel strategy for optimal placement of locally controlled voltage regulators in traditional distribution systems," *International Journal of Electrical Power & Energy Systems*, vol. 96, pp. 11–22, 2018.
- [27] M. A. X. de Lima, T. R. N. Clemente, and A. T. de Almeida, "Prioritization for allocation of voltage regulators in electricity distribution systems by using a multicriteria approach based on additive-veto model," *International Journal of Electrical Power & Energy Systems*, vol. 77, pp. 1–8, 2016.
- [28] N. Efkarpidis, T. De Rybel, and J. Driesen, "Optimal placement and sizing of active in-line voltage regulators in flemish LV distribution grids," *IEEE Transactions on Industry Applications*, vol. 52, no. 6, pp. 4577–4584, 2016.
- [29] A. S. Safigianni and G. J. Salis, "Optimum voltage regulator placement in a radial power distribution network," *IEEE Transactions on Power Systems*, vol. 15, no. 2, pp. 879–886, 2000.
- [30] A. Seppala, "Statistical distribution of customer load profiles," in *Proceedings 1995 International Conference on Energy Management and Power Delivery EMPD'95*, 1995, vol. 2, pp. 696–701.
- [31] F. Y. Ettoumi, A. Mefti, A. Adane, and M. J. R. E. Bouroubi, "Statistical analysis of solar measurements in Algeria using beta distributions," vol. 26, no. 1, pp. 47–67, 2002.
- [32] B. Renard and M. J. A. i. W. R. Lang, "Use of a Gaussian copula for multivariate extreme value analysis: some case studies in hydrology," vol. 30, no. 4, pp. 897–912, 2007.
- [33] J. Honerkamp, P. Weber, and A. J. N. P. B. Wiesler, "On the connection between the inverse transform method and the exact quantum eigenstates," vol. 152, no. 2, pp. 266–272, 1979.
- [34] C. S. Lai, Y. Jia, M. D. McCulloch, and Z. Xu, "Daily clearness index profiles cluster analysis for photovoltaic system," *IEEE Transactions on Industrial Informatics*, vol. 13, no. 5, pp. 2322–2332, 2017.
- [35] N. M. Razali and A. Hashim, "Backward reduction application for minimizing wind power scenarios in stochastic programming," in *2010 4th International Power Engineering and Optimization Conference (PEOCO)*, 2010, pp. 430–434: IEEE.
- [36] M. Baran and F. F. Wu, "Optimal sizing of capacitors placed on a radial distribution system," *IEEE Transactions on Power Delivery*, vol. 4, no. 1, pp. 735–743, 1989.
- [37] J. Zhao, Z. Xu, J. Wang, C. Wang, and J. Li, "Robust Distributed Generation Investment Accommodating Electric Vehicle Charging in a Distribution Network," *IEEE Transactions on Power Systems*, 2018.
- [38] R. R. Goncalves, J. F. Franco, and M. J. Rider, "Short-term expansion planning of radial electrical distribution systems using mixed-integer linear programming," *IET Generation, Transmission & Distribution*, vol. 9, no. 3, pp. 256–266, 2014.
- [39] P. P. Bedekar, S. R. Bhide, and V. S. J. W. T. o. P. S. Kale, "Optimum time coordination of overcurrent relays in distribution system using Big-M (penalty) method," vol. 4, no. 11, pp. 341–350, 2009.
- [40] I. I. J. Cplex, "V12. 1: User's Manual for CPLEX," *International Business Machines Corporation*, vol. 46, no. 53, p. 157, 2009.
- [41] G. Optimization, "Inc.,Gurobi optimizer reference manual, 2015," *Google Scholar*, 2014.
- [42] W. H. Kersting, "Radial distribution test feeders," in *Power Engineering Society Winter Meeting*, 2001, vol. 2, pp. 908–912.
- [43] *General Electric Company*. Available: <https://www.ge.com/>
- [44] *International Renewable Energy Agency (IRENA)*. Available: <https://www.irena.org/>
- [45] J. Huang, Z. Jiang, and M. Negnevitsky, "Loadability of power systems and optimal SVC placement," *International Journal of Electrical Power & Energy Systems*, vol. 45, no. 1, pp. 167–174, 2013.



Xu Xu (M'19) received the M.E. and Ph.D. degrees from The Hong Kong Polytechnic University, Hong Kong SAR, China, in 2016 and 2019, respectively. Dr. Xu is currently a Postdoctoral Fellow with the Department of Electrical Engineering, The Hong Kong Polytechnic University, Hong Kong SAR, China, and also a Visiting Scholar with the Department of Electrical and Electronic Engineering, Southern University of Science and Technology, Shenzhen, China. His current research interests include power system planning and operation, renewable power integration, energy management, and artificial intelligence application in power engineering.



Youwei Jia (M'15) received the B.Eng. and Ph.D. degrees from Sichuan University, China, in 2011, and The Hong Kong Polytechnic University, Hong Kong SAR, China, in 2015, respectively. From 2015 to 2018, he was a postdoctoral fellow at The Hong Kong Polytechnic University. He is currently an Assistant Professor with the Department of Electrical and Electronic Engineering, Southern University of Science and Technology, Shenzhen, China. His research interests include microgrid, renewable energy modeling and control, power system security analysis, complex network and artificial intelligence in power engineering.



Chun Sing Lai (M'19) received the B.Eng. (First Class Honours) in Electrical and Electronic Engineering from Brunel University London, UK and DPhil in Engineering Science from the University of Oxford, UK in 2013 and 2019, respectively. Dr Lai is currently a Lecturer at Department of Electronic and Computer Engineering, Brunel University London, UK and also a Visiting Academic with the Department of Electrical Engineering, Guangdong University of Technology, China. His current interests are in power system optimization, energy system modelling, data analytics, and energy economics for low carbon energy networks and energy storage systems.



Minghao Wang (M'18) received the B.Eng. (Hons.) degree in Electrical and Electronic Engineering from Huazhong University of Science and Technology, Wuhan, China, and University of Birmingham, Birmingham, U.K. in 2012, and the M.Sc. and the Ph.D. degree, both in Electrical and Electronic Engineering, from University of Hong Kong, Hong Kong SAR, China, in 2013 and 2017, respectively. Since 2018, he has been with the Department of Electrical Engineering, Hong Kong Polytechnic University, Hong Kong SAR, China. Currently, he is a

Research Assistant Professor in the Department of Electrical Engineering, the Hong Kong Polytechnic University. His research interests include power systems and power electronics.



Zhao Xu (M'06–SM'13) received the Ph.D. degree in Electrical Engineering from The University of Queensland, Brisbane, Australia, in 2006. From 2006 to 2009, he was an Assistant and later Associate Professor with the Centre for Electric Technology, Technical University of Denmark, Lyngby, Denmark. Since 2010, he has been with Hong Kong Polytechnic University. His research interests include demand side, grid integration of wind power, electricity market planning and management, and AI applications.